

Effect of brazing temperature on the shear strength of Inconel 600 joint

Tuan Zaharinie · Farazila Yusof · Mohd Hamdi ·
Tadashi Ariga · Raza Moshwan

Received: 20 June 2012 / Accepted: 25 April 2014 / Published online: 13 May 2014
© Springer-Verlag London 2014

Abstract In this study, Inconel 600 alloy was brazed by using Cusil ABA which is an active filler alloy in a high-vacuum condition under a pressure of 1×10^{-4} Pa. Three brazing temperatures (830, 865, and 900 °C) were chosen based on the solidus temperature of AgCuTi filler alloy in order to investigate the effects of these temperatures on the performance of the brazed joint. Brazing processes were carried out over a period of time (15 min) to ensure that the filler alloy was melted completely. The performance of the brazing process was evaluated in terms of bonding strength by shear test, whereas microstructural analysis was performed to investigate the bonding morphology. The results revealed that a maximum value of shear strength (223.32 MPa) was obtained at a brazing temperature of 865 °C compared with other temperatures. It was also observed morphologically that the highest shear strength was influenced by the formation of two reaction layers that crossed in the center of the brazed area due to interdiffusion effect of several constituents from the Inconel 600 alloy and active brazing filler.

Keywords Vacuum brazing · Brazing temperature · Inconel 600 · AgCuTi filler · Shear strength

1 Introduction

In the manufacturing industry particularly in joining, brazing is applied to join two materials using heat and filler metal with a melting temperature of above 450 °C. Two materials are joined by heating up to melting point of the filler metal in order to ensure that the molten filler flows via capillary action between the two mating surfaces. In this particular brazing process, alloying would occur by the diffusion of the molten brazing filler with the mating materials to form a metallurgical bond [1].

High-temperature brazing is very important and commonly employed in repairing and joining of nickel-based superalloys such as in aeroengine hot sections [2–5]. In this case, Inconel 600 is an austenitic type of nickel-based alloy (Ni-Cr-Fe) which is widely used in aeronautical, marine, and aerospace engineering due to its unique properties, one of them being that the alloy strength can be retained at high temperature [6, 7]. Furthermore, the formation of a stable passive oxide layer by chromium leads to excellent corrosion resistance in certain applications especially in oxidizing and sulfur-compounded environments. The high nickel content in the alloy provides superior corrosion resistance to some organic and inorganic compounds [8–10]. In practice, Inconel 600 alloy is commonly joined by diffusion brazing process. This process is a hybrid process with a combination of transient liquid phase (TLP) joining and diffusion bonding techniques [11, 12]. Besides, it is commonly employed due to its technological and economical advantages and in such cases, nickel-based alloys are normally selected as filler [13–16].

The selection of an appropriate brazing filler is significant in the brazing process as this affects the joining performance

T. Zaharinie (✉) · F. Yusof · M. Hamdi · R. Moshwan
Center of Advanced Manufacturing and Materials Processing,
Department of Engineering Design and Manufacture, Faculty of
Engineering, University of Malaya, 50603 Kuala Lumpur, Malaysia
e-mail: rinie34@gmail.com

F. Yusof
e-mail: farazila@um.edu.my

M. Hamdi
e-mail: hamdi@um.edu.my

R. Moshwan
e-mail: raza_moshwan2007@yahoo.com

T. Ariga
Department of Materials Science, School of Engineering, Tokai
University, 1117 Kitakaname, Hiratsuka-shi, Kanagawa 259-1292,
Japan
e-mail: ttariga@keyaki.cc.u-tokai.ac.jp

[17]. The eutectic composition of Ag-Cu-based filler alloy is often preferable due to its ductility and capability of limiting the increment of stresses during the brazing process. On the other hand, the type of brazing filler influences the selection of brazing temperature. As compared with Ni-based filler alloy that needed higher than 1,000 °C brazing temperature that is limited to be conducted, brazing using silver-based filler alloy promised a brazing temperature lower than 1,000 °C [18, 19]. It is noteworthy that the morphology and behavior of Inconel 600 tend to change with respect to annealing temperature especially at high temperature. Therefore, the selection of brazing temperature plays an important role to prevent formation of an intermetallic phase which is detrimental to the brazing strength [19, 20]. According to the theory during brazing, it is believed that several elements from Inconel 600 tend to react with the brazing filler during the process at high temperatures, which results in the formation of phases that influence the brazing strength of the alloy [1, 21].

Many researchers have been devoted on the diffusion brazing process, and there is a limited amount of literature which reports the vacuum brazing process [22, 23, 15]. Vacuum brazing offers a number of distinctive advantages over diffusion brazing, which include low residual stress in the brazed joint due to the use of a silver-based filler metal which acts as a buffer for stresses. Moreover, low pressure is required within the bonding zone during the joining process [19]. In such cases, there is a lack of detailed literature which focuses on the investigation and analysis of vacuum-brazing Inconel 600 alloy using Cusil ABA [19]. Therefore, in this research, the authors aim to investigate the effect of vacuum brazing temperature on the shear strength of Inconel 600 containing 1.75 wt.% active brazing filler. The analysis is focused on exploring the effects of several elements and/or phases formed by the reaction of Inconel 600 with the active brazing filler.

2 Experimental details

Inconel 600 alloy was supplied by Azbil-Yamatake Corporation, Japan, and composition of the as-received alloy is presented in Table 1. The Inconel 600 alloy plate was prepared with a base dimension of $4 \times 25 \times 25 \text{ mm}^3$ and a top dimension of $4 \times 8 \times 8 \text{ mm}^3$ for the experiments. Cusil ABA (supplied by Wesgo Metals, USA) was selected as the filler and its chemical composition is 63Ag-1.75Ti-35.25Cu. Cusil ABA filler was prepared with a dimension of $0.05 \times 10 \times 10 \text{ mm}^3$. The sample arrangement of brazing Inconel 600 to Inconel 600 in the clamp system is illustrated in Fig. 1.

The brazing processes were carried out in a Tokyo Vacuum furnace under a vacuum condition with a pressure of $1 \times 10^{-4} \text{ Pa}$. Such vacuum condition is required to ensure that the brazing sample is free from undesirable contaminants between the mating materials. For each brazing cycle, the

Table 1 Composition of as-received Inconel 600 (in wt.%)

| C | Si | Mn | P | S | Ni | Cr | Fe | Cu |
|------|------|------|-------|-------|------|-------|------|------|
| 0.02 | 0.09 | 0.21 | 0.005 | 0.001 | 74.4 | 16.32 | 8.87 | 0.08 |

heating and cooling rates were kept constant at 5 and 3 °C/min, respectively. The brazing temperature was set at three different temperatures (830, 865, and 900 °C) for a duration of 15 min. The process was repeated three times with two samples for each brazing temperature. The heating profile at brazing temperatures of 830, 865, and 900 °C is shown graphically in Fig. 2.

Shear tests were carried out in an Instron Universal Testing Machine with a load cell (model 3369). A diagram of the clamp system is shown in Fig. 3 and the crosshead speed is set to 0.5 mm/min. The shear test was repeated three (3) times to ensure the reliability of the joined samples.

Three samples were prepared for each brazing temperature for microscopic evaluation. Each sample was sectioned using a diamond saw cutter, and the sample was precisely polished in order to investigate the microstructural behavior at the cross section. An optical microscope (model Olympus) equipped with get IT software was employed to examine the interfaces present in the brazing seam. Finally, the specimens were examined in detail using a scanning electron microscope (SEM; model Quanta 2000) with Energy Dispersive Spectroscopy (EDS) from Oxford Instruments equipped with INCA software to analyze the elements and phases present in the brazing area and interfaces. The mapping analysis was delivered by SEM (Hitachi; model SU8000). After shear test, the broken surface of Inconel 600 alloy was examined by X-ray diffraction (XRD) analysis. The phases left at the surfaces were further analyzed by XRD (CuK_α).

3 Results and discussion

3.1 Shear strength and microstructure analyses

Figure 4 shows the shear strength of the brazed joint for three brazing temperatures (830, 865, and 900 °C). The results of the seizure experiment showed that shear strengths of 177,

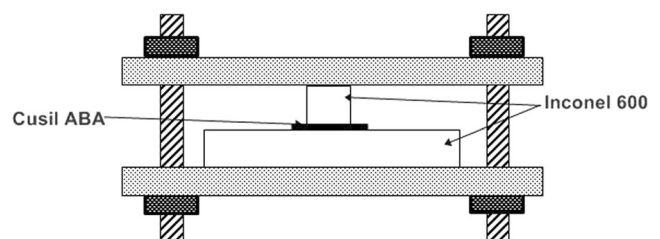
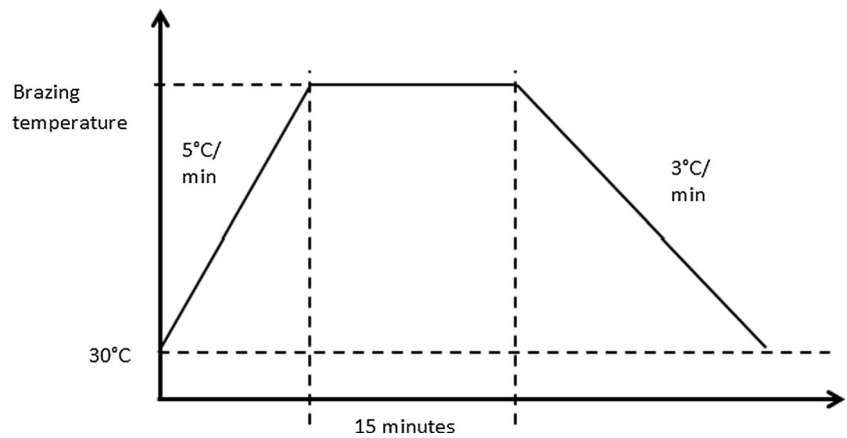


Fig. 1 Sample arrangement of brazing Inconel 600 to Inconel 600 in clamp system

Fig. 2 Heating profile at brazing temperatures of 830, 865, and 900 °C



223.32, and 188.8 MPa were obtained at brazing temperatures of 830, 865, and 900 °C, respectively. The shear value is comparable with that obtained by Yue et al. (123–188 MPa) for vacuum brazing of titanium alloy to stainless steel and that obtained by Shiue et al. (89.7–200 MPa) for infrared brazing of Cu with Ti [24, 19]. Their researches deal with the AgCuTi brazing filler and the shearing area mostly occurred in the brazing alloy. It shall be highlighted that the error bars in the graph indicate that the data is relatively precise. For all brazing parameters, the fracture mode was observed to be in brittle behavior with small percentage of ductility (approximately 20 %). The morphology relation between the failure modes will be discussed in the next section.

Microstructural analysis was performed in order to investigate the effect of brazing temperature on the shear strength of the brazed joint in morphological view. Figure 5 shows the SEM micrographs of the brazing area under a magnification of $\times 2,000$ for each brazing temperature. It can be observed that a

good physical contact and metallurgical bond was established at the Inconel 600 joint. It is also apparent that the joint is free from microvoids and porosity. The brazing filler reacts with the Inconel 600 alloy during the brazing process. It is worthy to note again that the brazing material used in this study is eutectic Cusil ABA with a thickness of 50 μm .

Measurements of the brazing filler thickness show that the initial gap of 50 μm is reduced to about 50 % after brazing, and it can be seen that 50 % of the brazing filler reacts and dissolves in the Inconel 600 alloy. From Fig. 5, there is also a formation of two reaction layers for both sides in the brazed area due to the same base materials, and the observed big-sized copper-rich phase indicated that the brazing has been conducted in a very slow cooling. This suggests that the phenomenon influences the strength of the brazed joint of Inconel 600 alloy. Furthermore, it can be clearly observed that the white area with small contents of Fe and Ni was reduced with increasing brazing temperature. Mapping analysis by SEM indicates that the white area was identified to be Ag-rich phase. The situation is agreeable with other literature on titanium to stainless steel, and the reduction of brazing thickness has been influenced by the increase in overflow of the Ag-rich liquid during brazing and the depletion of copper during melting of filler alloy [25, 19]. An investigation by

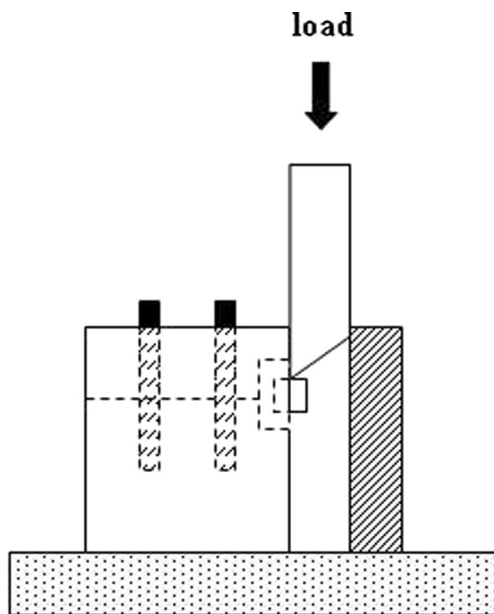


Fig. 3 Shear test clamping system

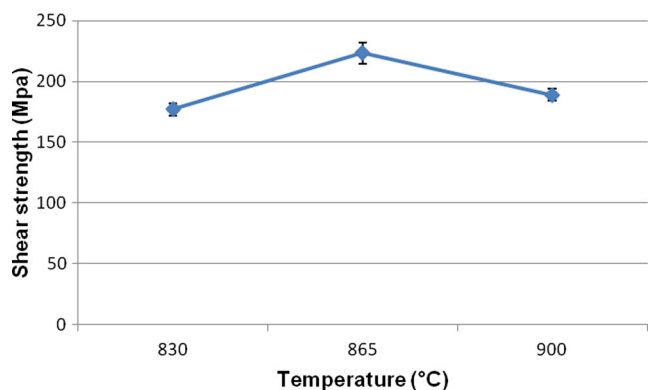
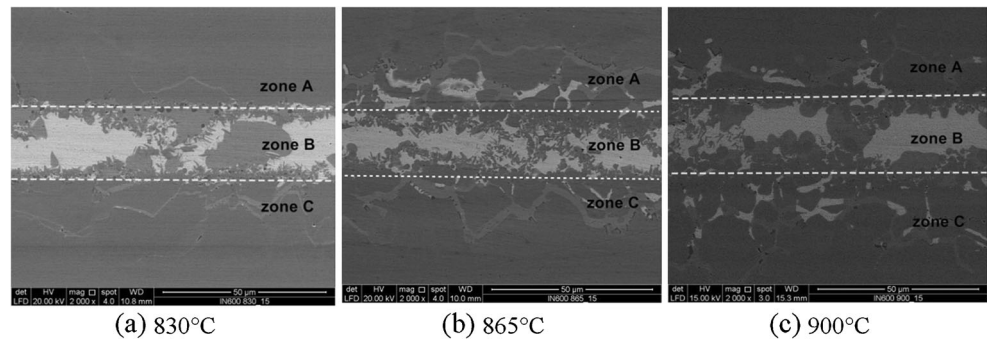


Fig. 4 Shear strength of brazed joint for three brazing temperatures (830, 865, and 900 °C)

Fig. 5 SEM micrographs of brazing area under a magnification of $\times 2,000$ for brazing temperatures of **a** 830, **b** 865, and **c** 900 °C



Mandal et al. has proven that the thickness of Ag-Cu is important to accommodate the stress during brazing of ceramics, which is also applicable for brazing metals. However, in this study, the Ag-Cu area was reduced with the increase of brazing temperatures. This phenomenon exhibits the major brittleness fracture mode occurring in all brazing condition [26].

The shearing area was observed by using an optical microscope under a magnification of $\times 500$, and the results are shown in Fig. 6. It is apparent from Fig. 6 that the shearing area occurred in the center of the brazing zone. This evidence suggests that shearing occurred mostly in Ag-rich or Cu-rich areas between the two reaction layers. As shown in Fig. 6, the reaction layer (shown in gray) is more prominent compared to other areas.

It is well documented that the reaction layers influence the bonding strength of the brazed joint. During shearing, the weakest area was located at the center of the brazed area which was a Ag-rich phase. For the lowest temperature in this study, the Ag-rich-phase area was the widest and the formation of two continuous reaction layers mostly occurred nearby Inconel 600. Hence, the brazing temperature was insufficient for more elements from Inconel 600 to diffuse towards the center of brazing filler. This phenomenon was proven by XRD analysis in Fig. 7a that conducted on the surface of broken

area. The XRD analysis shows that at the lowest temperature, only the elements of silver (Ag), copper (Cu), chromium (Cr) and iron chromium (FeCr) were detected. However, at 865 °C and 900 °C (Fig. 7b and 7c), iron (Fe) started to influence the bonding due to more elements from Inconel 600 such as Ni, Cr, and Fe diffused and reacted with the brazing filler. Consequently, the bonding-affected zone begins to increase and the Ag-rich-phase area was reduced. At this stage, the high affinity of Ni, Cr, and Fe elements towards Ti contained within the brazing filler results in the formation of the reaction layer crossing in the center of the brazing area. This reaction layer obstructed the shearing stress which occurs at the joint. Finally, at the highest brazing temperature of 900 °C, the reaction layer begins to form non-continuously nearby the interface of Inconel 600 and the thickness of the bonding-affected zone was increased. The reaction layers that crossed in the center of the brazing area also become globules and discontinuous. This suggests that the continuous reaction layer played an important role to increase the shear strength of the brazed joint at 865 °C compared with 830 and 900 °C.

3.2 Brazed area, reaction layer, and element analyses

Figure 8 shows the mapping analysis of the sample at 865 °C. It can be observed that the reaction layer mainly consisted of Ti and Ni. This evidence may suggest the significance of Ti content in brazing filler alloy that influences the bonding strength. It is worthy to note that the behavior of formation of the reaction layer was influenced by the active brazing temperature. Analysis has been done and converted into a sketch as shown in Fig. 9.

Starting at 830 °C (Fig. 9a), it can be clearly observed that the formation of the reaction layer occurred continuously in close proximity to the Inconel 600 side zone compared to the center zone of the brazing area. This analysis revealed that the interaction between the brazing filler and Inconel 600 alloy has not yet begun since the liquidus state of filler alloy was at 815 °C. It can be observed that the active element Ti remains in the brazing filler along with a high content of Ag and a small amount of Cu.

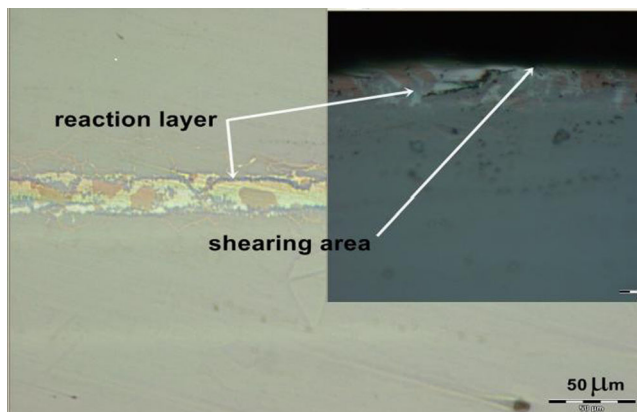


Fig. 6 Shearing area observed under an optical microscope with a magnification of $\times 500$

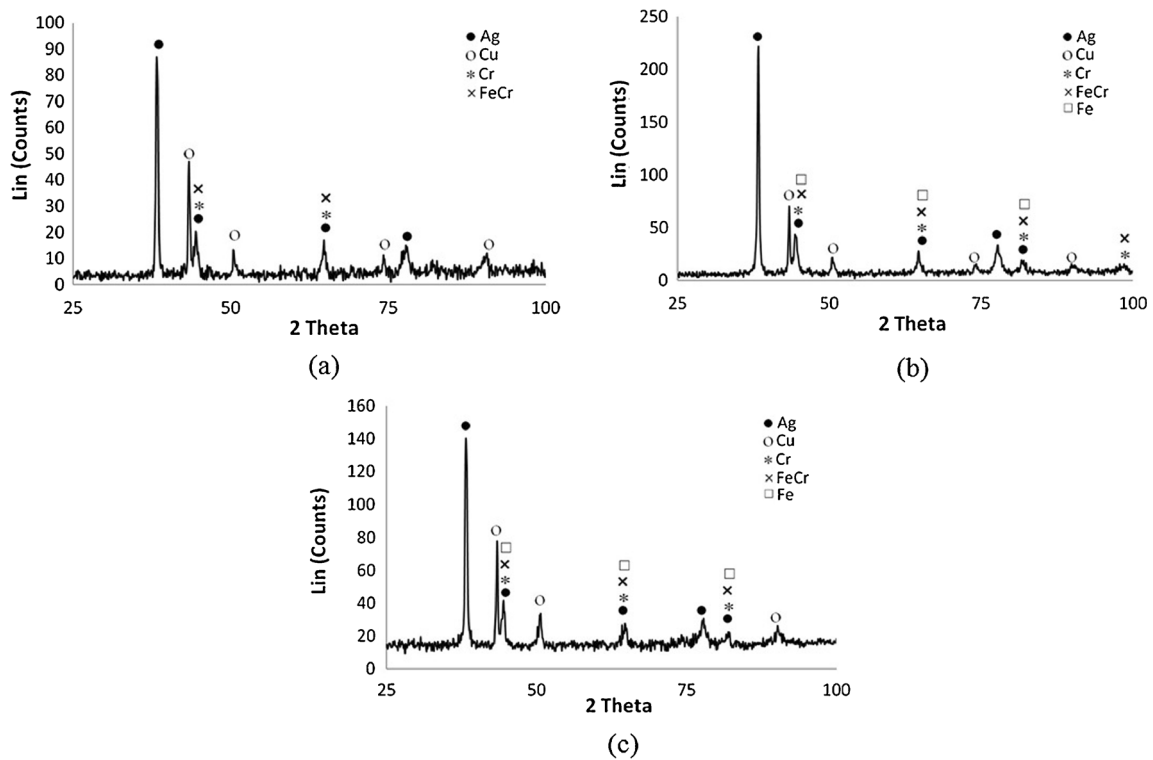
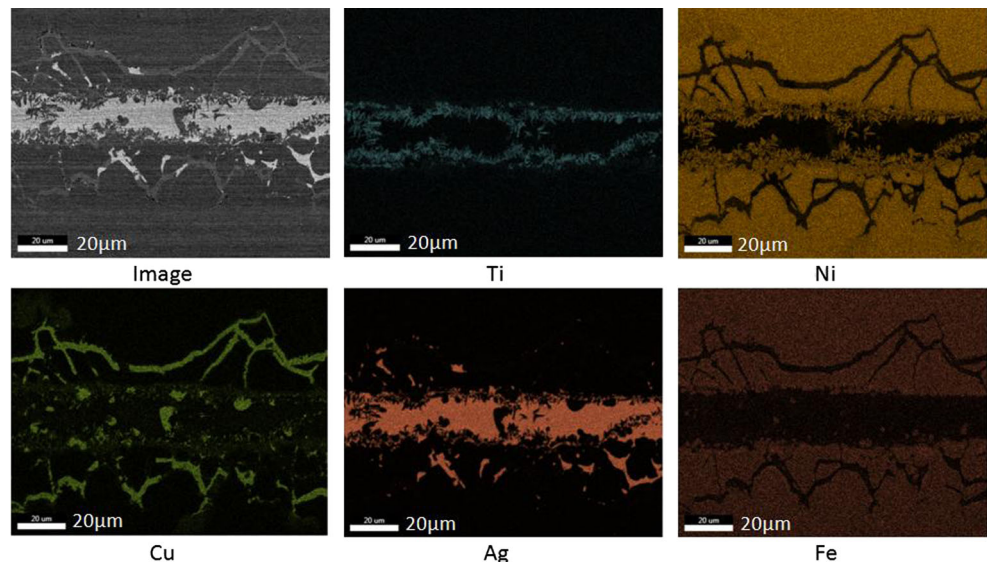


Fig. 7 XRD analysis at the side of broken specimen after shear test for a 830, b 865, and c 900 °C

Figure 9b shows that at 865 °C, 20 % of the reaction layer begins to cross the center zone of the brazing area that results in a maximum shear strength of 223.32 MPa. This can be explained by the bonding morphological behavior. From Fig. 10, three zones (marked in white font) could be clearly observed: zones A, B, and C. Zones A and C are the bonding-affected zones, and both zones exhibit similar reactions due to the fact that the parent material is similar in both sides. Formation of the bonding-affected zone was influenced by

interdiffusion of alloying elements from molten brazing filler alloy and dissolution of the base metal during brazing. It was also observed that a non-isothermal solidified zone occurred in zone B due to the copper-rich island which could be detected in all brazing temperatures. The formation of zone B was influenced by the solidification of liquid filler alloy over the brazing period of time. During this time, interdiffusion occurred between the brazing filler and Inconel 600 alloy [27, 12]. However, due to the formation of a eutectic-like

Fig. 8 Mapping analysis of sample at 865 °C by SEM



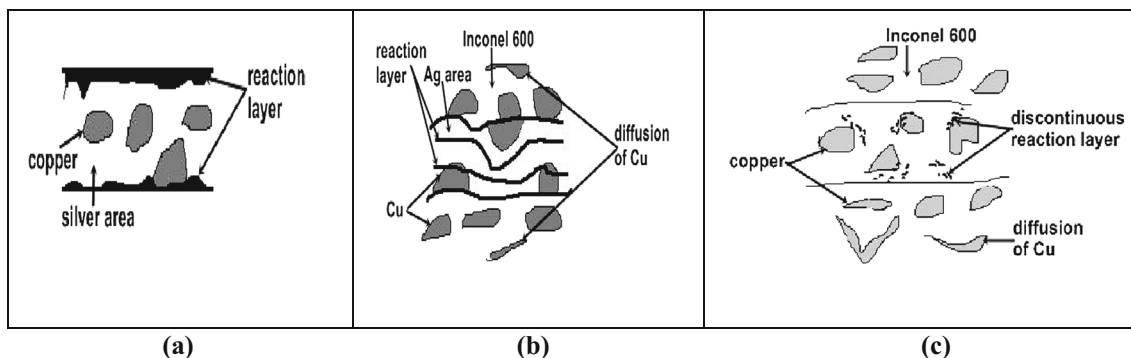


Fig. 9 Formation of the reaction layer by the influence of different brazing temperatures

structure of the Cu-rich island, it is suggested that the formation of the Cu-rich island occurred due to the incomplete isothermal solidification of molten filler alloy at the bonding temperature. According to this theory, diffusion between nickel (Ni) and chromium (Cr) from Inconel 600 and the brazing filler occurred during non-isothermal solidification. During the brazing process, the filler alloy melted to form a liquid phase and reacted with the base metal, which resulted in interdiffusion of alloying elements between the base metal and molten brazing filler alloy. The compositions of the elements within the reaction layer are different, and the Ni, Cr, and Fe elements begin to diffuse into the brazing filler alloy at this temperature. Consequently, this leads to the formation of the reaction layer crossing to the center of the brazing area as well as a reduction of the filler alloy thickness. On the other hand, almost the same diffusion occurred at 900 °C; however, the reaction layer started to become discontinuous and the

bonding-affected zone grew gradually. The growing of the bonding-affected zones at 900 °C did not influence the brazing strength of Inconel 600.

Further investigations were carried out by SEM-EDS analyses to demonstrate the interdiffusion behavior of several elements of the brazed joint. Figure 10 and Table 2 show the results of SEM-EDS analyses for a brazing temperature of 865 °C. From the results, it can be seen that at point A, the reaction layer consisted of a high percentage of Ni and Cr compared to point B. At point C, the amounts of Ni and Cr are the highest compared to other elements. From the results, it can be deduced that Ni, Fe, and Cr from Inconel 600 are diffused into the brazing filler. Since Ti has a very high affinity towards Ni and Fe, the role of Ti from the brazing filler metal is very important to improve the strength of the brazed joint of Inconel 600 alloy.

From the microstructural and shear strength test data analyses, it is proven that the shear strength reaches its maximum value of 223.32 MPa at 865 °C, whereas the shear strength at 830 and 900 °C showed very poor performance over the same brazing period of time. For this particular research, it is worthy to point out that, in the case of brazing of Inconel 600, the brazing temperature 865 °C is much more effective, convenient, and reliable than the brazing temperatures of 830 and 900 °C over the same brazing period of time. It can be also suggested that, to get a more optimized value of brazing temperature, further research may be conducted in the future around 865 °C.

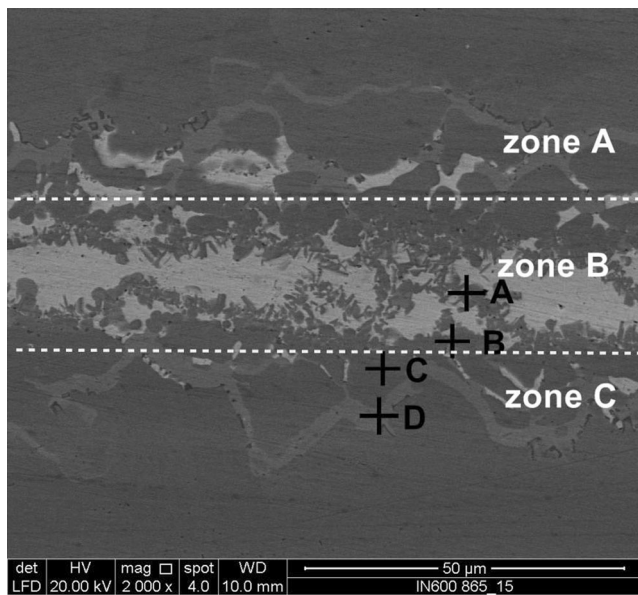


Fig. 10 Point analysis of SEM-EDS and three zones marked for brazing interfaces at a brazing temperature of 865 °C

Table 2 EDS data analysis according to point analysis in Fig. 10 (in wt.%)

| | Ti | Cr | Fe | Ni | Cu | Ag |
|---|------|-------|------|-------|-------|-------|
| A | 4.49 | 12.38 | 7.74 | 54.9 | 13.1 | 7.36 |
| B | 8.8 | 6.0 | 4.0 | 46.56 | 13.18 | 21.45 |
| C | 0.41 | 15.81 | 9.04 | 69.51 | 3.12 | 2.11 |
| D | 0.3 | 9.61 | 5.36 | 39.72 | 42.51 | 2.49 |

4 Conclusions

In this research, the effect of brazing temperature on the shear strength of the brazed joint of Inconel 600 for the same brazing time of 15 min was investigated successfully. The summary of the current research could be concluded as follows:

- a) The highest shear strength of 223.32 MPa was obtained at a brazing temperature of 865 °C compared with 830 and 900 °C which could be applicable in many areas of the joining field.
- b) The brazing time of 15 min is not enough for the molten filler alloy to react with Inconel 600 at 830 °C due to the fact that the liquidus state of filler alloy is at 815 °C. However, by increasing the brazing temperature up to 865 °C, the reaction began and two continuous reaction layers started to cross in the center, hence increasing the strength of the bonding by resisting crack propagation. Again, by increasing the brazing temperature up to 900 °C, the reaction layer started to become granulated and discontinuous which causes the reduction in shear strength.
- c) Formation of the two reaction layers crossing in the center of the brazed area was affected by the diffusion of some elements from Inconel 600 alloy (especially Ni) with the Ti-molten brazing filler during brazing which significantly influenced the bonding strength of the brazed joint.

Acknowledgments The authors greatly acknowledge the members of Azbil-Yamatate Corporation for supplying the Inconel 600 alloy for investigation in this research and University of Malaya Kuala Lumpur for financial support via Postgraduate Research Grant (PPP Grant No.: pv058/2011a).

References

1. Humpston G, Jacobson DM (1993) Principles of soldering and brazing. ASM International, USA
2. Wu XW, Chandel RS, Seow HP, Li H (2001) Wide gap brazing of stainless steel to nickel-based superalloy. *J Mater Process Technol* 113(1–3):215–221. doi:10.1016/s0924-0136(01)00596-9
3. Srinivasan G, Bhaduri AK, Ray SK, Shankar V (2008) Vacuum brazing of Inconel 600 sleeve to 316L stainless steel sheath of mineral insulated cable. *J Mater Process Technol* 198(1–3):73–76. doi:10.1016/j.jmatprotec.2007.06.069
4. Shan JG, Ren JL, Khorunov VF (2002) Repairing of the defects of the engine vanes of an aeroplane by light beam brazing. *J Mater Process Technol* 121(1):23–26. doi:10.1016/s0924-0136(01)01187-6
5. Zhang Q, He X, Li Y (2011) Microstructure evolution and mechanical properties of a nickel-based honeycomb sandwich aged at 900 °C. *Mater Sci Eng A Struct* 530:202–207. doi:10.1016/j.msea.2011.09.075
6. Madhusudhana Reddy G, Srinivasa Murthy CV, Srinivasa Rao K, Prasad Rao K (2009) Improvement of mechanical properties of Inconel 718 electron beam welds—influence of welding techniques and postweld heat treatment. *Int J Adv Manuf Technol* 43:671–680. doi:10.1007/s00170-008-1751-7
7. Imran M, Mativenga PT, Gholinia A, Withers PJ (2011) Evaluation of surface integrity in micro drilling process for nickel-based superalloy. *Int J Adv Manuf Technol* 55:465–476. doi:10.1007/s00170-010-3062-z
8. Al-Rubaie KS, Godefroid LB, Lopes JAM (2007) Statistical modeling of fatigue crack growth rate in Inconel alloy 600. *Int J Fatigue* 29(5):931–940. doi:10.1016/j.ijfatigue.2006.07.013
9. Kwon J-d, Park D-k, Woo S-w, Yoon D-h, Chung I (2010) A study on fretting fatigue life for the Inconel alloy 600 at high temperature. *Nucl Eng Des* 240(10):2521–2527. doi:10.1016/j.nucengdes.2010.05.013
10. Hu HX, Zheng YG, Qin CP (2010) Comparison of Inconel 625 and Inconel 600 in resistance to cavitation erosion and jet impingement erosion. *Nucl Eng Des* 240(10):2721–2730. doi:10.1016/j.nucengdes.2010.07.021
11. Idowu OA, Richards NL, Chaturvedi MC (2005) Effect of bonding temperature on isothermal solidification rate during transient liquid phase bonding of Inconel 738LC superalloy. *Mater Sci Eng A Struct* 397(1–2):98–112. doi:10.1016/j.msea.2005.01.055
12. Yuan X, Kim MB, Kang CY (2009) Characterization of transient-liquid-phase-bonded joints in a duplex stainless steel with a Ni–Cr–B insert alloy. *Mater Charact* 60(11):1289–1297. doi:10.1016/j.matchar.2009.05.012
13. Arafin MA, Medraj M, Turner DP, Bocher P (2007) Transient liquid phase bonding of Inconel 718 and Inconel 625 with BNi-2: modeling and experimental investigations. *Mat Sci Eng A Struct* 447:125–133. doi:10.1016/j.msea.2006.10.045
14. Wikstrom NP, Egbewande AT, Ojo OA (2008) High temperature diffusion induced liquid phase joining of a heat resistant alloy. *J Alloys Compd* 460(1–2):379–385. doi:10.1016/j.jallcom.2007.06.066
15. Egbewande AT, Chukwukaeme C, Ojo OA (2008) Joining of superalloy Inconel 600 by diffusion induced isothermal solidification of a liquated inserted metal. *Mater Charact* 59:1051–1058. doi:10.1016/j.matchar.2007.08.023
16. Miyazawa Y, Ariga T (1992) Brazing of Inconel 600 and SUS304 stainless steel with used of rapidly solidified nickel-base brazing foil. *Mater Trans* 33(5):509–518
17. Sabetghadam H, Hanzaki AZ, Araee A, Hadian A (2010) Microstructural evaluation of 410 SS/Cu diffusion-bonded joint. *J Mater Sci Technol* 26(2):163–169. doi:10.1016/S1005-0302(10)60027-8
18. Kang S-W, Chen Y-T, Liu H-P (2005) Brazing diffusion bonding of micro-nickel cylinders and SUS-316 stainless steel. *J Mater Process Technol* 168(2):286–290. doi:10.1016/j.jmatprotec.2005.02.234
19. Yue X, He P, Feng JC, Zhang JH, Zhu FQ (2008) Microstructure and interfacial reactions of vacuum brazing titanium alloy to stainless steel using an AgCuTi filler metal. *Mater Charact* 59(12):1721–1727. doi:10.1016/j.matchar.2008.03.014
20. Li H-x, He P, Lin T-s, Pan F, Feng J-c, Huang Y-d (2012) Microstructure and shear strength of reactive brazing joints of TiAl/Ni-based alloy. *Trans Nonferrous Met Soc* 22(2):324–329. doi:10.1016/s1003-6326(11)61178-3
21. Jadoon AK, Ralph B, Hornsby PR (2004) Metal to ceramic joining via a metallic interlayer bonding technique. *J Mater Process Technol* 152(3):257–265. doi:10.1016/j.jmatprotec.2003.10.005
22. López B, Gutiérrez I, Urcola JJ (1992) Study of the microstructure obtained after diffusion bonding inconel 625 to low alloy steel by hot uniaxial pressing or hiping. *Mater Charact* 28(1):49–59. doi:10.1016/1044-5803(92)90028-g
23. Jalilian F, Jahazi M, Drew RAL (2006) Microstructural evolution during transient liquid phase bonding of Inconel 617 using Ni–Si–B filler metal. *Mat Sci Eng A Struct* 423(1–2):269–281. doi:10.1016/j.msea.2006.02.030

24. Shiue RK, Wu SK, Chan CH (2004) The interfacial reactions of infrared brazing Cu and Ti with two silver-based braze alloys. *J Alloys Compd* 372(1–2):148–157. doi:10.1016/j.jallcom.2003.09.155
25. Elrefaey A, Tillmann W (2009) Correlation between microstructure, mechanical properties, and brazing temperature of steel to titanium joint. *J Alloys Compd* 487(1–2):639–645. doi:10.1016/j.jallcom.2009.08.029
26. Mandal S, Ray AK, Ray AK (2004) Correlation between the mechanical properties and the microstructural behaviour of Al_2O_3 -(Ag-Cu-Ti) brazed joints. *Mat Sci Eng A Struct* 383(2):235–244. doi:10.1016/j.msea.2004.06.002
27. Yuan X, Yun Kang C, Kim MB (2009) Microstructure and XRD analysis of brazing joint for duplex stainless steel using a Ni-Si-B filler metal. *Mater Charact* 60(9):923–931. doi:10.1016/j.matchar.2009.03.004